Proceedings of the 9th U.S. National and 10th Canadian Conference on Earthquake Engineering
Compte Rendu de la 9ième Conférence Nationale Américaine et
10ième Conférence Canadienne de Génie Parasismique
July 25-29, 2010, Toronto, Ontario, Canada • Paper No 1506

NONLINEAR ANALYSIS OF T-SHAPED CONCRETE WALLS SUBJECTED TO MULTI-DIRECTIONAL LOADING

J. D. Waugh[1] and S. Sritharan[2]

ABSTRACT

Non-rectangular concrete walls are widely used in the design of buildings to resist lateral loads due to wind and earthquake loading. Presented in this paper are nonlinear analyses of T-shaped concrete walls subjected to unidirectional and multidirectional loading using fiber-based beam-column elements. Key results of the analyses are compared to the experimental data to show that fiber-based beam-column elements can be used to adequately capture the response of nonrectangular walls under multidirectional cyclic loads. The analysis results were within 5-15% of the measured global response for the post-test analysis and within 10-20% for the pre-test analysis. Local responses were captured satisfactorily by the pre-test analyses and more accurately by the post-test analyses.

Introduction

Engineers and architects often use structural walls as part of the primary lateral force resisting system for buildings due to their high in-plane strength and stiffness that enable them to resist large lateral forces induced by loads such as wind and earthquakes. The high in-plane strength and stiffness of walls typically limit the lateral interstory drifts, thus resulting in reduced damage to both structural and nonstructural elements. Another common practice in building design is to use non-rectangular walls as they can form functional features such as stairwells and elevator core while serving as the primary lateral force resisting system. Therefore, understanding both the behavior and response predictability of non-rectangular walls is as important as that of rectangular concrete walls to ensure dependable structural performance of the buildings during large earthquake events.

In current seismic design practice (e.g., IBC 2006, ACI 318-05, Eurocode 8), structures are designed to respond nonlinearly when subjected to large ground accelerations resulting from moderate to large earthquakes. This approach allows for smaller, more economical structural elements to be used in buildings, while making them less sensitive to the actual acceleration history of the input earthquake motions. Consequently, a number of challenges ensue when analyzing the expected seismic response of these structures. The extent of such challenges is dependant on the capabilities of the analysis tools and the chosen modeling techniques.

[1]Structural Engineering Intern, HNTB Corporation, Westbrook, ME 04092
[2]Wilson Engineering Associate Professor, Dept. of Civil, Construction and Environmental Engineering, Iowa State University, Ames, IA 50011

This paper presents a modeling approach to accurately simulate the global and local behavior of T-shaped reinforced concrete walls using beam-column elements with fiber sections. An open source finite element program (OpenSees) is used for this purpose and the models and analysis results are validated utilizing large-scale wall test data from a PreNEESR project (Brueggen, 2009). The topics covered in this paper are a summary of experimental testing, the key modeling issues in accurately simulating the response of non-rectangular structural walls, a general description of the analytical models, the analysis of the two NEES T-walls and comparison of the analysis results with the experimental response.

Summary of Experimental Testing

Fig. 1a shows details of NTW1, which had a 228.6 cm (90 in.) long web with a 182.9 cm (72 in.) wide flange. This wall was 7.32 m (24 ft) tall and had wall thickness of 15.2 cm (6 in.) for the flange and web. NTW1 was a 50% scale specimen of a T-wall designed by a practicing engineer for a six story office building in Los Angeles, California (Brueggen *et al.* 2007). NTW1 represented the standard practice of the design of structural walls.

The loading protocol for NTW1 subjected the wall to displacements parallel to the web, parallel to the flange, and in directions with components parallel to the web and the flange to follow specific lateral displacement paths. These special load cases included a pentagon shaped path at approximately 50% of the first yield displacement, and an hourglass shaped path at 2% lateral drift and were intended to provide complex load paths to adequately verify the accuracy of the analysis models in simulating the wall response; these two paths are shown in Fig. 2. During testing, a constant axial load ratio of 4% of $f'_c A_g$ (i.e., axial load of 829.6 kN (186.5 k)) was maintained at the top of the wall to maintain the gravity load effects. NTW1 modeled only four stories of the six-story high wall and thus a moment was applied to make the effective height of the shear force 792.5 cm (312 in.) above the base of NTW1. More complete information on the load path for NTW1 can be found in Brueggen (2009) and Waugh (2009). Upon completion of the hourglass shaped load path at 2% drift, NTW1 experienced failure of the web tip. Upon deconstruction of NTW1, it was discovered that a number of hoops in the web tip open up leading to a loss of confinement of the concrete and buckling of the longitudinal reinforcement. Additionally, concrete crushing was observed outside the boundary element. NTW1 was then tested in the flange direction to 2.5% drift without failure. Failure of the flange tips occurred at the 3% drift level displacements; this was also due to buckling of the longitudinal reinforcement.

The second of two T-walls tested at the UMN MAST facility, referred to as NTW2, is shown in Fig. 1b. NTW2 was designed to improve the response observed for NTW1 by preventing the transverse hoops from failing at the 2% drift level. NTW2 was also a half-scale specimen and had the same gross dimensions as NTW1. However, this wall specimen modeled only the bottom two stories of the six-story prototype wall and incorporated significantly different details for the longitudinal and transverse reinforcement than NTW1. NTW2 maintained nearly the same total area of steel in the flange as NTW1. However, they differed in that NTW1 had the longitudinal steel reinforcement concentrated in the flange tips as recommended in the current design practice (e.g., ACI 318-05), while NTW2 had the steel almost evenly distributed across the flange width. The decision to distribute the flange steel was to maintain the width and spacing of flexural cracks evenly across the flange width. Additionally, the boundary element containing the confinement

reinforcement in the web tip was extended based on the analysis of NTW1. To prevent opening of the hoops and cross-ties in the confinement regions, the hoops were arranged so the hooks were as further away than near the web tip, thereby reducing the demand on the confinement splices. Finally, the continuous longitudinal reinforcement used in NTW1 was replaced in NTW2 with lap-spliced longitudinal reinforcement with the splices extending upward from the bottom of the first floor level. Splicing at the first floor level was chosen to minimize the influence of the splice on development of the plastic hinge.

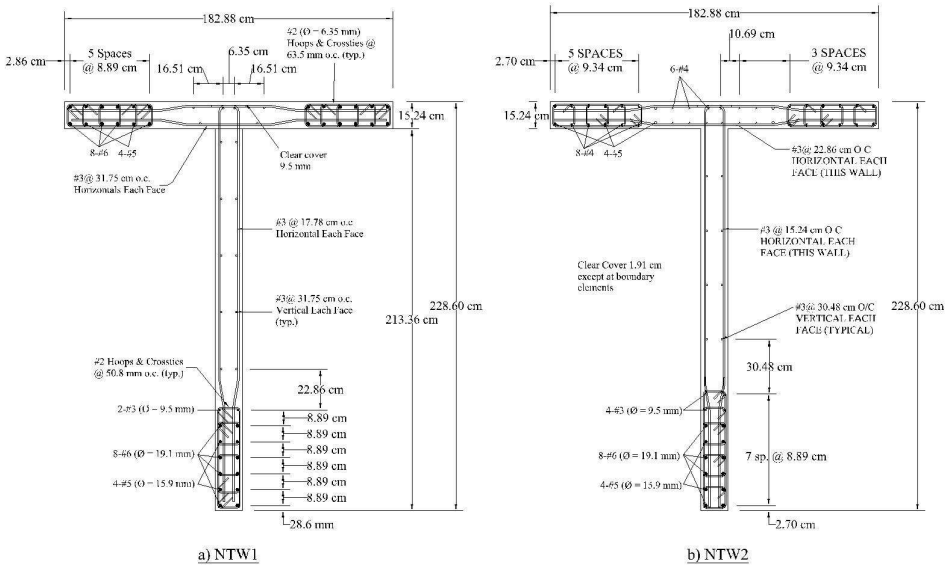

Figure 1. T-wall sections and reinforcement details.

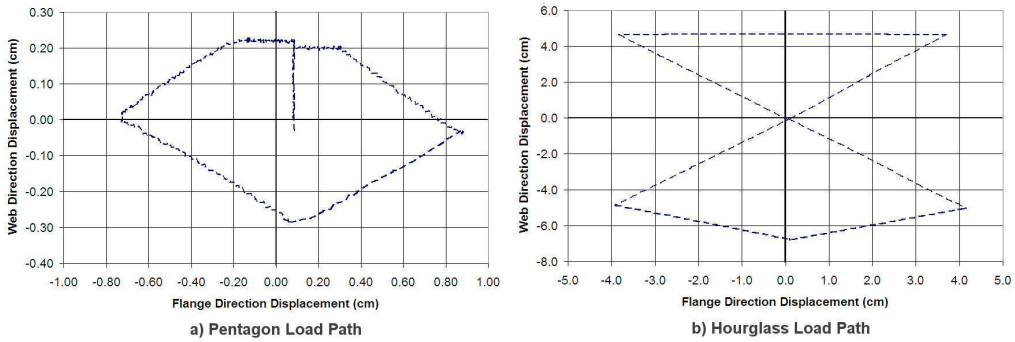

Figure 2. T-wall sections and reinforcement details.

The loading protocol for NTW2 was the same as for NTW1 so the effect of the distributed steel and other modifications could be evaluated without having load path dependant effects interfere. The shear-to-moment ratio at the base of the wall was also maintained. However, the axial load was increased to 895.4 kN (201.3 k) to include the weight of the third and fourth stories of the wall that were not included in NTW2, resulting in the same axial load ratio at the base of the two wall test units. Overall, the experimental performance of the NTW2 was better than NTW1 and reached a lateral drift of 2.5% in the web direction, and 3% in the flange direction without experiencing any strength degradation. The improved performance of the wall was attributed to the enhanced details adopted for NTW2.

Key Issues in Non-rectangular Wall Simulation

A well-designed wall subjected to lateral loads will experience both shear and flexural deformations. The analysis presented herein has focused on slender walls with large aspect ratios (i.e., the ratio of the height to the length of the wall), whose lateral load behavior is dominated by flexure. The response of this type of structural walls is influenced by nonlinear material behavior, axial load effects including P-delta, the extent of strain penetration, shear deformation effects, shear-flexure interaction, and shear lag effects. Each of these components needs to be included in the analytical model to accurately simulate both global and local responses. These issues are discussed in greater detail in Waugh (2009).

In addition to the aforementioned issues, the response of a flexural dominated wall may be influenced by the presence of lap splices in the critical regions (Waugh *et al.* 2009), anchorage failure of the longitudinal reinforcement, shear failure due to yielding of the transverse reinforcement, web crushing, and/or horizontal sliding of the base of the wall (Park and Paulay 1975). However, these additional issues may be avoided with proper design and detailing of a wall.

Description of Analytical Model

The fiber-based beam-column approach was chosen in this study to simulate the response of two T-walls under multi-directional loads due to its computational efficiency, but the aforementioned challenges are adequately addressed as described later in this section. The models were developed in OpenSees using force-based beam-column elements (Taucer *et al.* 1991), as these elements have been shown to better simulate the length and rotation of the plastic hinge region, which are important for accurate prediction of the flexural behavior (Neuenhofer and Filippou 1997). These beam-column elements included five integration points along the member length, where the strains in all fibers in the section were calculated. The cross-section for the beam-column elements modeling the wall included the concrete fibers and the steel fibers representing the longitudinal reinforcement as per the details of the wall. The confinement effects of the transverse reinforcement were accounted for by appropriately defining the hysteretic behavior of the concrete using the model proposed by Chang and Mander (1994) with modifications introduced by Waugh (2009). The longitudinal reinforcement was modeled using a Mennegotto-Pinto hysteretic model (Mazzoni 2004) with isotropic strain hardening material which was available in OpenSees.

The fiber-based beam-column element in OpenSees does not include the effects of shear deformation, requiring it to be handled separately. A uniaxial material model was used to describe the shear force vs. shear deformation of the beam-columns modeling the T-walls. The envelope of the uniaxial material model as defined to capture the shear deformation included a point corresponding to the nominal yield and corresponding decrease in stiffness. This causes the inelastic shear deformation to occur simultaneously with the inelastic flexural deformation, following the observations reported by Massone and Wallace (2004). The shear material was then aggregated onto the defined fiber section and acted as a shear spring in parallel with the beam-column element.

The strain penetration effects on the wall response were simulated with a zero-length element using the strain penetration model developed and introduced into OpenSees by Zhao and Sritharan (2007). This model quantifies the total bar slip at an element end due to strain penetration

along the bar into an adjoining member to the bar stress at the element end under monotonic or cyclic loading. The section of the zero-length element was identical to the section used for the beam-column elements modeling the wall; however, the material for the fibers modeling the longitudinal reinforcement was changed from the Mennegotto-Pinto (Mazzoni 2004) steel model to the strain penetration model of Zhao and Sritharan (2007). Additionally, the uniaxial behavior of concrete fibers was modified according to the recommendations of Zhao and Sritharan to account for the additional confinement effects expected from the foundation. The boundary conditions for the zero-length element were to fully fix the bottom node against all deformations, while restraining the top node against translation in all three directions and torsion. The top node was then utilized as the bottom node of the beam-column element modeling the first floor of the wall for the 3D analysis.

To simulate the effects of shear lag, a modification to the determination of fiber strains at the section level was made in OpenSees. This was achieved by creating a new fiber section based on the previously available fiber section in OpenSees and modifying the tension strain distribution across the flange due to "flange-in-tension" loading. The equations used to account for shear lag effects are presented in Waugh (2009). The shear lag equations are second order equations that account for the length and thickness of the flange; one equation represents reinforcement concentrated in the flange tips, while the other represents reinforcement distributed across the flange.

Both T-walls were subjected to multidirectional loading, with both a displacement and a moment applied at the top of the walls during testing. The moment was applied to give a specific shear-to-moment ratio at the base of the walls as the walls did not model the entire height of the prototype wall. To ensure that the proper shear-to-moment ratio was applied in the simulation, the displacements at an imaginary control point located at a height of 792.5 cm (312 in.) above the base of the wall, which eliminated the need to impose any moments to the analysis models. Furthermore, displacements for the analyses were specified for both the lateral translational DOFs to model the multidirectional nature of the testing. Any displacement pattern could be applied to these wall models by specifying the appropriate component values for the translation DOFs.

All wall analyses were conducted in OpenSees using a Krylov-Newton solver (Mazzoni 2004) to increase the efficiency of the analysis by not reforming the stiffness matrix at each iteration and using subspace acceleration. The norm of the displacement increment was used to determine when a converged solution was achieved. The P-Δ effects were included in the analysis using a geometric transformation option available in OpenSees.

Test Specimen NTW1

The OpenSees model for NTW1 was developed following the general concept described above, using a beam-column element for each of the four floor levels. The analysis presented here for this wall is based on a post-test analysis. The wall cross-section for the beam-column element was discretized using fibers that were approximately 6.35 mm by 6.35 mm (0.25 in. by 0.25 in.). The shear deformation was aggregated onto the fiber section, with a separate material model for the two orthogonal directions at each floor level. A Pinching4 material model was used to model the shear response parallel to the web and flange for the first floor, while an origin-centered hysteretic

material model was used for the second and third floor shear responses parallel to the web and flange as nonlinearity in shear response was limited at the upper floors. The fourth floor shear response was simulated using an elastic material model for the response parallel to both the web and flange.

Figs. 3a and 3b show the global force-displacement response at the top of fourth floor level in the flange and web directions, respectively. The overall response of the wall was well captured by the OpenSees model. Figs. 4a,b and 4c,d show the force-displacement response in the flange and web directions for the pentagon and hourglass displacement paths. These cycles show the ability of the analysis to capture complex multidirectional displacement paths. The peak forces were accurately simulated by the analysis, within approximately 10% of the measured values for displacements parallel to the flange or the web, and within approximately 15% for the multidirectional displacements. The lateral stiffness of the wall was well captured in virgin territory as well as during unloading and reloading.

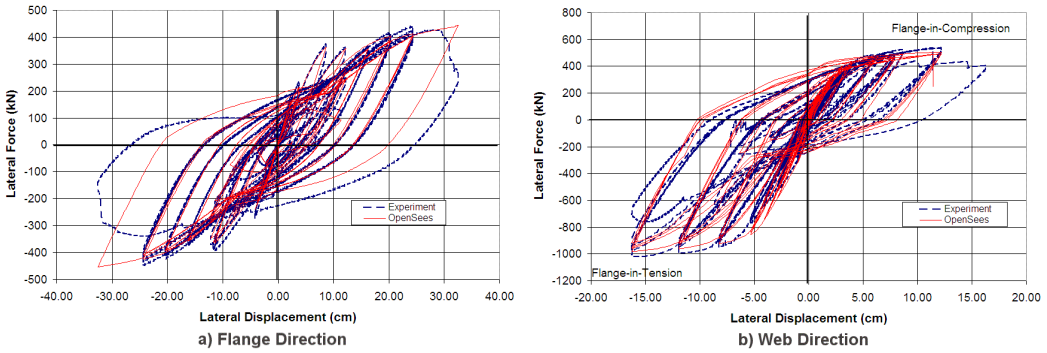

Figure 3. NTW1 force-displacement response in the flange and web directions.

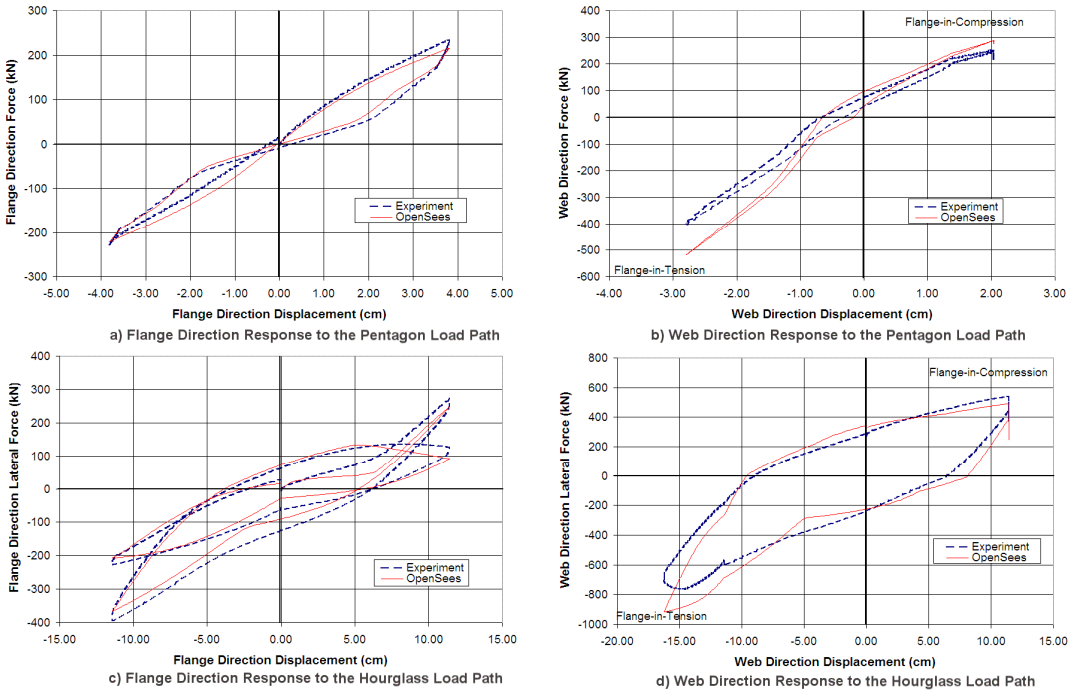

Figure 4. NTW1 force-displacement responses for multidirectional displacement paths.

Figs. 5a, b, c, and d show the curvature near the wall base in the web and flange directions. The experimental curvature was determined from strain gauges located 15.2 cm (6 in.) above the base of the wall. This location was selected for comparison because more reinforcement was instrumented at this height and it also minimized any confinement effects of the foundation. In the flange-in-compression and flange-in-tension directions, OpenSees simulated the strain profile and location of the neutral axis satisfactorily. The strain profile for the flange-in-tension direction shows that strains above 0.005 mm/mm (0.005 in./in.) were predicted outside the web boundary element for lateral displacements corresponding drifts of above 1.0%, which is consistent with the observed concrete crushing at that location. For the flange direction, the curvature is again well simulated by the analysis. However, only one displacement level is shown because the majority of the flange direction loading occurred after failure of the web tip and the gauges had failed.

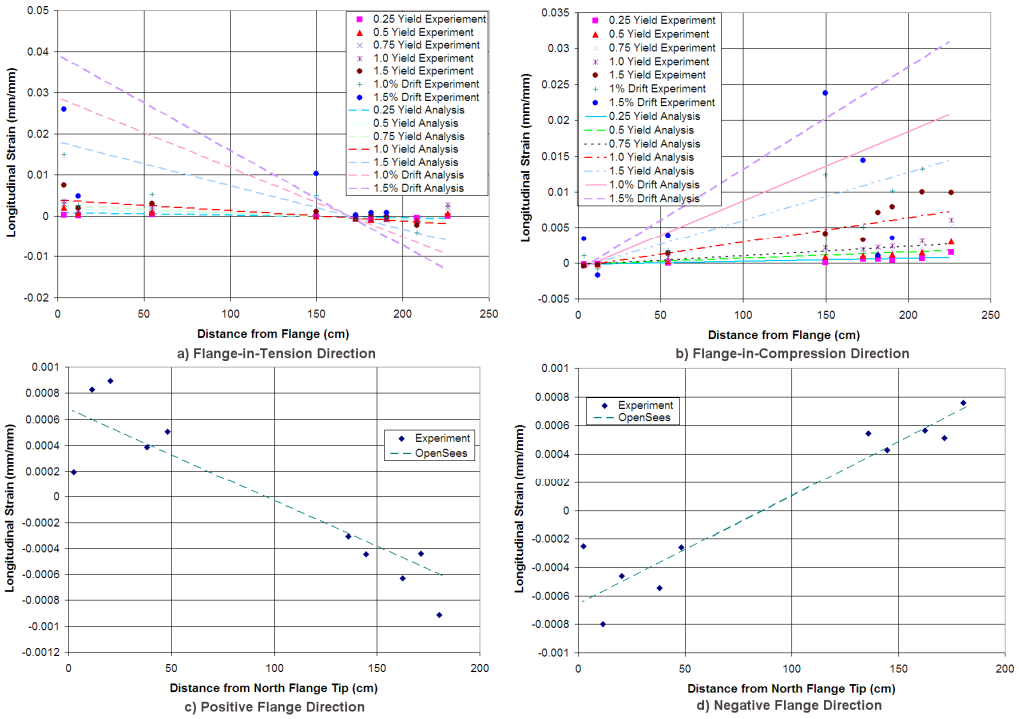

Figure 5. Curvature of NTW1 in the web and flange directions.

Test Specimen NTW2

The OpenSees model for NTW2 was modeled following the procedure used for NTW1, using a beam-column element for each of the two floor levels. However, the model for NTW2 was used to predict the response of NTW2 prior to the test. The wall cross-section for the beam-column element was again discretized using fibers that were approximately 6.35 mm by 6.35 mm (0.25 in. by 0.25 in.). The shear deformation was again aggregated onto the fiber section, but because NTW2 was analyzed prior to the test, the shear contributions were modeled based on the response of NTW1.

The lateral force-displacement responses predicted in the flange and web directions are shown in Figs. 6a and b, respectively. The experimental response in each direction shows the average of the recorded string potentiometer displacements measured at the flange tips and the force

resistance recorded by actuator load cells during the test. The analytical response was taken from the lateral displacement recorded at the node representing the second floor level of NTW2 while the force resistance was established from the member forces at the bottom end of the beam-column element modeling the wall at the first floor level. Fig. 6a shows the flange direction response was overpredicted at approximately 3.0 cm (1.2 in.) by about 25%. However, the rest of the response is predicted within 10%. As seen in Fig. 6b, the web direction response was generally well captured by the analytical model until NTW2 experienced strength degradation due to buckling of the longitudinal reinforcement in the web tip boundary element at a lateral displacement of -8.4 cm (-3.3 in.). A good agreement between the experimental and simulated force-displacement responses are observed in terms of the force resistance in the flange-in-compression loading direction, the unloading/reloading stiffness, and the residual displacements after unloading from peak lateral displacements. The force resistance in the flange-in-tension loading direction was underestimated by the analysis by approximately 5%.

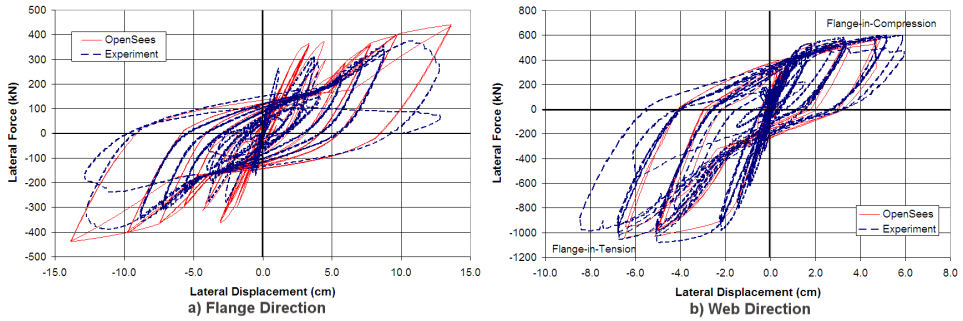

Figure 6. NTW2 force-displacement responses in the flange and web directions.

Figs. 7a,b and 7c,d show the force-displacement response in the flange and web directions for the pentagon and hourglass displacement paths. The peak forces, as well as the unloading and reloading stiffnesses, were accurately captured in the web direction. Between the peaks, the force in the flange-in-compression loading direction was underpredicted by approximately 20% at the largest difference being at about 1.25 cm (–0.5 in.) of displacement. In the flange direction, the overall shape and stiffness of the response loops were satisfactorily predicted given the complexity of the load path. The flange direction response was more accurately predicted in the positive direction; however, in the negative displacement direction, the force was overestimated by as much as 40%. This discrepancy was likely caused by not accurately simulating the accumulated damage in the flange direction that was present prior to beginning this specific load path.

Figs. 8a and b shows the curvatures in the web direction for NTW2. As with NTW1, the experimental curvature was determined from strain gauges located 15.2 cm (6 in.) above the base of the wall. As before, in the flange-in-compression and flange-in-tension directions, OpenSees simulated the strain profile and location of the neutral axis with sufficient accuracy. No gauges in the flange direction loading survived, and thus comparison of strain distribution was not possible in that direction for NTW2.

Conclusions

The beam-column elements with fiber sections adequately simulated the response of the T-walls subjected to multi-directional loading. The force-displacement response at the top of the wall

was satisfactorily captured by the post-test analysis conducted for NTW1 and by the pre-test analysis of NTW2. In each of these models, an improved concrete hysteretic model and a strain penetration model, which have been implemented into OpenSees, were incorporated. In addition, the wall models accounted for the shear lag effects and shear deformation as accurately as possible within the current capabilities of OpenSees.

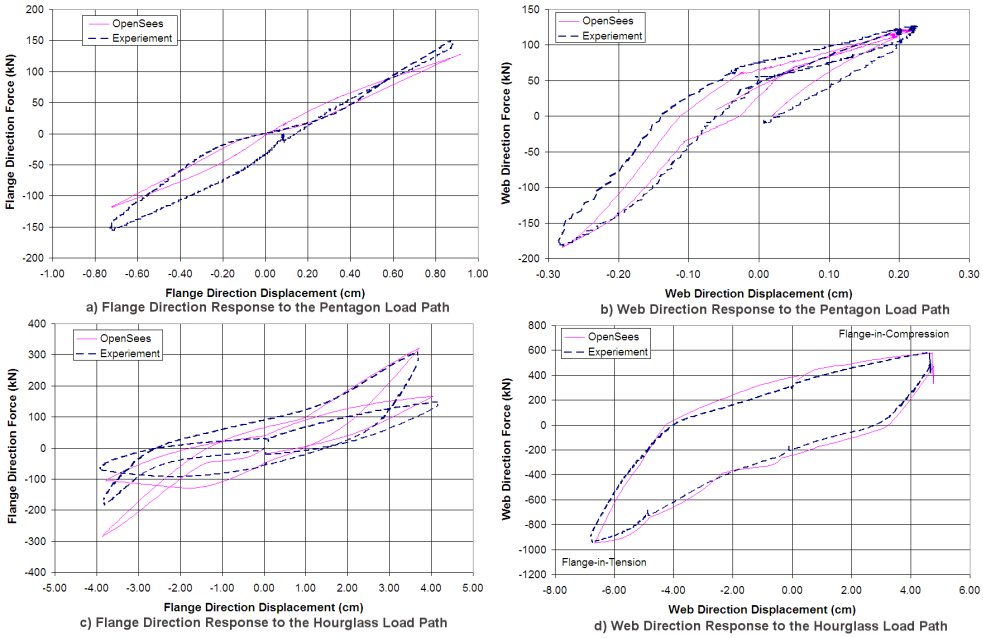

Figure 7. NTW2 force-displacement response for multidirectional displacement paths.

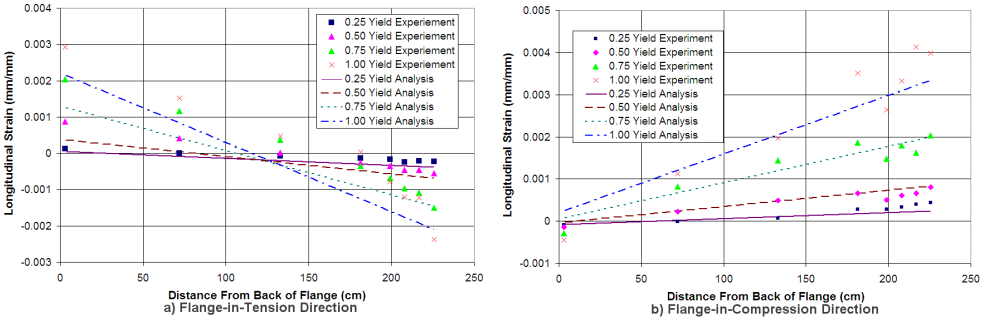

Figure 8. Curvature of NTW2 in the web direction.

The model of NTW1 yielded a very good simulation of the force-displacement response, giving forces within 5 to 10% of the measured lateral force resistance for a given displacement in both the flange and web directions. The hourglass and pentagon load paths chosen to investigate the wall behavior to complex multi-directional loads were well simulated by the analysis model, in terms of the lateral force resistance and stiffness. Under this complex loading, the lateral force resistance was well simulated except for the peak in the web direction where the peak resistance was over estimated by approximately 20%.

The model for NTW2 was able to capture the measured lateral force within 10–15% of the measured values, with one region in the flange direction at approximately 3-5 cm. (1.2 – 2.0 in.)

where the force resistance was over predicted by approximately 25%. The lateral force resistance to the multidirectional loading was generally well simulated with the response typically within 15% of the measured values; except for peaks in the negative flange direction, 30% over predicted.

While the method used in this study to analyze T-walls subjected to multi-directional loading yielded adequate simulation of the experimental response, a few limitations of the analysis should be noted and appropriate improvements should be made in the future. First, only well detailed, flexurally dominated walls were investigated. Second, the shear behavior of the walls was taken from the measured shear deformation response of NTW1. More research and development is needed to properly predict the shear deformation behavior. Finally, the shear lag had a different effect on the strain distribution in the flanges of NTW1 and NTW2. While the distribution functions used for this analysis can be used, great care should be given in determining the appropriate function, which depends on the distribution of the flange reinforcement.

References

American Concrete Institute Committee 318, 2005. *Building Code Requirements for Structural Concrete,* Farmington Hills, Michigan.

Brueggen, B., 2009. Performance of T-shaped reinforced concrete shear walls under multi directional loading, *Ph.D Thesis,* University of Minnesota.

Brueggen, B., Waugh, J., Aaleti, S., Johnson, B., French, C., Sritharan, S., Nakaki, S., 2007. Tests of Structural Walls to Determine Deformation Contributions of Interest for Performance Based Design, *Proceedings of the 2007 Structures Congress*, American Society of Civil Engineers, Reston, VA.

Chang, G., and Mander, J., 1994. Seismic Energy Based Fatigue Damage Ananlysis of Bridge Columns: Part 1 – Evaluation of Seismic Capacity, *NCEER Technical Report No. NCEER-94-0006,* State University of New York.

International Code Council, 2006. *International Building Code (IBC),* Virgina.

Massone, L.M., and Wallace, J.W., 2004. Load Deformation Response of Slender Reinforced Concrete Walls, *ACI Structural Journal,* 101 (1) 103-113.

Mazzoni, S., McKenna, F., Scott, M.H., Fenves, G.L., 2004. Open System for Earthquake Engineering Simulation Ver. 1.6.0, *Pacific Earthquake Engineering Research Center,* University of California, Berkeley.

Neuenhofer, A., and Filippou, F.C., 1997. Evaluation of Nonlinear Frame Finite-Element Models, *ASCE Journal of Structural Engineering,* 123 (7), 958-966.

Park, R., and Paulay, T., 1975. *Reinforced Concrete Structures*, New York: John Wiley and Sons.

Taucer, F., Spacone E., Filippou. F.C., 1991. A Fiber Beam-Column Element for Seismic Response Analysis of Reinforced Concrete Structure,. *Report No. UCB/EERC-91/17,* Earthquake Engineering Research Center, College of Engineering, University of California, Berkeley.

Thomsen, J., and Wallace, J., 1995. Displacement-Based Design of RC Structural Walls: An Experimental Investigation of Walls with Rectangular and T-Shaped Cross-Sections, *Report to the National Science Foundation*, Department of Civil Engineering, Clarkson University.

Waugh J., 2009. Nonlinear Analysis of T-shaped concrete walls subjected to multi-directional displacements, *Ph.D Thesis,* Iowa State University.

Waugh, J., Aaleti, S., Sritharan, S., and Zhao, J., 2009. Nonlinear Analysis of Rectangular and T-shaped Concrete Walls, ISU-ERI-Ames Report ERI-09327, Iowa State University.

Zhao, J., and Sritharan, S., 2007. Modeling of Strain Penetration Effects in Fiber-Based Analysis of Reinforced Concrete Structures, *ACI Structural Journal,* 104 (2) 133-141.